

Targeting adenocarcinoma and enzalutamide-resistant prostate cancer using the novel anti-androgen inhibitor ADA-308

SHAGHAYEGH NOURUZI^{1,2*}, FRASER JOHNSON^{1*}, SAHIL KUMAR¹, OLENA SIVAK¹,
NAKISA TABRIZIAN^{1,2}, MILLA KOISTINAH³, ANU MUONA³ and AMINA ZOUBEIDI^{1,2}

¹Vancouver Prostate Centre, Vancouver, BC V6H 3Z6, Canada; ²Department of Urology, Faculty of Medicine, University of British Columbia, Vancouver, BC V5Z 1M9, Canada; ³Aranda Pharma Ltd., 70210 Kuopio, Finland

Received February 13, 2024; Accepted July 4, 2024

DOI: 10.3892/or.2024.8791

Abstract. Prostate cancer (PCa) is the leading cause of cancer-related death among men worldwide. PCa often develops resistance to standard androgen deprivation therapy and androgen receptor (AR) pathway inhibitors, such as enzalutamide (ENZ). Therefore, there is an urgent need to develop novel therapeutic strategies for this disease. The efficacy of ADA-308 was evaluated through *in vitro* assessments of AR activity and cell proliferation, alongside *in vivo* studies. ADA-308 has emerged as a promising candidate, demonstrating potent inhibition of AR-sensitive adenocarcinoma as well as ENZ-resistant PCa cell lines. The results of the study revealed that ADA-308 effectively blocked AR activity, including its nuclear localization, and inhibited cell proliferation *in vitro*. Furthermore, ADA-308 demonstrated notable efficacy *in vivo*, with a robust antitumor response in ENZ-resistant models. These findings establish the role of ADA-308 as a potent AR inhibitor that overcomes resistance to AR-targeted therapies and highlights its potential as a novel therapeutic approach in advanced PCa management.

Introduction

Prostate cancer (PCa) is the second most common cancer among men (1), and remains a major health challenge owing to it rising incidence and mortality rates (2). According to the World Health Organization, PCa is the fourth most common cancer globally, with ~1.4 million new cases and ~375,000 deaths reported in 2020 alone (3), emphasizing the urgent

need for improved prevention and diagnostic strategies. PCa progression is highly dependent on the androgen receptor (AR), which fuels tumor growth and survival (4). The mainstream treatment for localized and metastatic PCa is androgen deprivation therapy (ADT), which reduces circulating androgens and abrogates AR signalling to prevent disease progression (5,6). Despite treatment with ADT, AR signalling is re-activated in most patients and these patients evade therapy-induced castration conditions, resulting in the recurrence of PCa as castration-resistant PCa (CRPC) (7,8). Re-activation of AR signalling occurs despite low levels of androgens in CRPC. Thus, the AR plays a central role in mediating tumour survival. Treatment with second-generation androgen receptor pathway inhibitors (ARPIs) such as enzalutamide (ENZ; also known as MDV3100), abiraterone and apalutamide has been successful in managing CRPC tumors and increasing patient survival (9,10). The competitive non-steroidal AR antagonist, ENZ, improves survival in patients with non-metastatic CRPC (11,12). Despite its potent AR pathway inhibition, the benefits of ENZ are short-lived, and patients inevitably progress to metastatic CRPC (mCRPC) (13,14). ARPI resistance represents a clinical challenge due to the lack of third-line treatment options. Taken together, these findings highlight the urgent need for new therapeutic options for refractory patients with mCRPC, including those resistant to second-generation ARPIs.

The progression of CRPC to ARPI resistance may be mediated through adaptive responses that activate AR-signaling via other pathways. A number of underlying mechanisms exist, including the alteration of AR signalling via i) aberrant glucocorticoid receptor upregulation (15), ii) AR splice variants (such as AR-V7) (16,17), iii) AR gene mutations (18), iv) an increase in AR expression (19), and v) enhancer amplification and duplication of the AR gene (20-22). CRPC predominantly remains AR⁺ (23,24), and a subset of ENZ-resistant models display AR reactivation (25,26), which demonstrates the importance of AR signalling in mCRPC and indicates that it remains a therapeutic vulnerability.

In the present study, the efficacy of ADA-308 was explored, as a possible rigorous benchmark against established anti-androgens, such as ENZ and darolutamide (ODM-201) (27). The mechanism of action of ADA-308 was investigated, particularly in terms of its AR inhibition activity in both AR-sensitive

Correspondence to: Dr Amina Zoubeydi, Vancouver Prostate Centre, 2660 Oak Street, Vancouver, BC V6H 3Z6, Canada
E-mail: azoubeydi@prostatecentre.com

*Contributed equally

Abbreviations: ENZ, enzalutamide; ARPIs, androgen receptor pathway inhibitors; PCa, prostate cancer; CRPC, castration-resistant PCa; ENZR, enzalutamide-resistant; Adeno, adenocarcinoma

Key words: prostate cancer adenocarcinoma, ARPIs, treatment-resistance, enzalutamide resistance

adenocarcinoma (Adeno) and ENZ-resistant cell models. Furthermore, the ability of ADA-308 to inhibit AR nuclear translocation and its impact on proliferation *in vitro* and on tumor growth *in vivo* were examined to establish its potential as an anti-androgen therapeutic option.

Materials and methods

Compound. ADA-308 was synthesized by Aranda Pharma Ltd. and manufactured by Jubilant Chemsys Ltd. ADA-308 boasts a notable purity level of 99.8%, signifying its high quality and consistency. The batch no. J763-Z01220-083 identifies the compound used in the present study.

Cell lines and cell culture treatments. Cell lines and cell culture treatments were maintained under standard conditions of 37°C and 5% CO₂. The LNCaP cell line was obtained from ATCC. 49C^{ENZ^R} (49C enzalutamide-resistant) and 49F^{ENZ^R} (49F enzalutamide-resistant) were generated from LNCaP cells, as previously detailed by our group (26,28). LNCaP and LNCaP-driven cell lines were cultured in RPMI-1640 media (Gibco; Thermo Fisher Scientific, Inc.; cat. no. 11875093) supplemented with 5% FBS (Gibco; Thermo Fisher Scientific, Inc.; cat. no. A3160701). ENZ-resistant cell lines were also cultured in 10 µmol/l ENZ. In addition, when indicated, cell lines were treated with 10 µmol/l ENZ or 10 µmol/l ADA-308 (Aranda Pharma Ltd.). For hormone stimulation with synthetic androgen, cells were treated with 10 nM R1881 (MilliporeSigma; cat. no. 965-93-5).

In vivo study. The animal experiments adhered to protocols approved by The Animal Care Committee at The University of British Columbia (Vancouver, Canada; approval no. A16-0246; approval date, 12/15/2016). Mice were housed in ventilated cages (4 mice per cage) under controlled conditions, including constant humidity (25-27%) and temperature (21-22°C), with a 12-h light-dark cycle. The mice were provided with unrestricted access to rodent chow diet and water and experiments on the mice began between 6-8 weeks of age. At the experimental or humane endpoint, mice were euthanized using an inhalant anesthetic (3% isoflurane) followed by carbon dioxide (50% of the cage volume per min). A secondary accepted physical method of euthanasia (decapitation) was performed to prevent revival. For castration, 2.5% isoflurane vaporizer and 2 l/min oxygen were used for anesthesia, providing both the induction and maintenance doses. A total of 12 mice were assigned per treatment group. The mice weighed ~20 g at the start of the study and were supplied by Envigo.

Male athymic mice were castrated and allowed to recover from surgery for 3 days. Then, 2x10⁶ 49F^{ENZ^R} cells were inoculated twice, once per site on the right and left flanks for the first *in vivo* study using 25 or 50 mg/kg ADA-308 and once on the right site for the second study using 12.5 or 25 mg/kg ADA-308. The mice were recovered for 3 days then administered 10 mg/kg ENZ daily until the tumor volume reached 200 mm³. Next, ENZ (10 mg/kg) was either continued (ENZ group) or switched to vehicle, ADA-308 at 12.5, 25 or 50 mg/kg twice a day (BID), or ODM-201 (Orion Pharmaceuticals Corporation) at 50 mg/kg BID. All treatments were administered orally (gavage) and all *in vivo* studies utilized a common vehicle,

a 2% Tween-0.5% carboxymethyl cellulose sodium salt solution. The tumor volumes were measured three times per week in a blinded fashion and calculated using the formula: Volume=[π (length x width x height)]/6. Recruitment was conducted in 10 cycles, the length of ENZ treatment ranging from 19 to 52 days. Mice were sacrificed at predetermined time points after treatment, when the tumor volume reached 2,000 mm³, when tumors reached >10% of the body weight or the body weight loss was >15%, whichever came first. The maximum long diameter of a single tumor was 21 mm and the maximum sum of the long diameter of both the left and right tumors in a single mouse was 33.5 mm. The maximum sum of the tumor volume of both the left and right tumors in a single mouse was 2,425 mm³. While the humane endpoint was set at a tumor volume of 2,000 mm³, the individual mouse in question that exceeded the tumor size belonged to the ENZ treatment group and had a tumor volume of 1,462 mm³ at the 2.5-week time point. Therefore, the mouse was not sacrificed at that time. By the 3-week time point, when tumors were measured again, the tumor volume had grown beyond the endpoint, resulting in a measurement of 2,425 mm³, at which point the mouse was then sacrificed.

Western blotting. Proteins were extracted from cells cultured *in vitro*. The cells were washed once with 1X PBS and subsequently lysed using RIPA buffer (Thermo Fisher Scientific, Inc.; cat. no. PI89901) enriched with a 1X concentration of cOmplete EDTA-free protease inhibitors cocktail (Roche Diagnostics; cat. no. 11836170001) and phosphatase inhibitors (PhosSTOP; Roche Diagnostics; cat. no. 4906845001). Following protein quantification using the BCA protein assay (Thermo Fisher Scientific, Inc.; cat. no. 23225), the samples were subjected to a 5-min boiling step in 4X SDS sample buffer. The 4X SDS sample buffer contained 8-10% SDS, 200 mM Tris-HCl (pH 6.8), 40% glycerol, 0.02% Bromophenol Blue and 5% β -mercaptoethanol. Equal amounts of protein (40 µg per lane) were resolved by SDS-PAGE using 10% polyacrylamide gels. The proteins were transferred onto PVDF membranes, then the membranes were blocked with Odyssey Blocking Buffer (LI-COR Biosciences; cat. no. 15590545) at room temperature for 30 min and probed with primary antibodies at the specified dilutions overnight at 4°C. The membranes were washed three times with 1X TBST (2% Tween-20) for 10 min, then probed with the appropriate secondary antibody for 1 h at room temperature. The membranes were washed three times with 1X TBST for 10 min before visualization using a LI-COR Odyssey Scanner. The immunoblotting utilized the following antibodies: AR (clone D6F11; 1:1,000; Cell Signaling Technology, Inc.; cat. no. 5153) and prostate-specific antigen (PSA; clone D6B1; 1:5,000; Cell Signaling Technology, Inc.; cat. no. 5365), with Vinculin (clone hvin-1; 1:25,000; Cell Signaling Technology, Inc.; cat. no. 4650) serving as the loading control. The secondary antibodies included IRDye 800CW donkey anti-rabbit (1:10,000; LI-COR Biosciences; cat. no. 926-32213). Uncropped western blots are shown in Fig. S1.

Reverse transcription-quantitative PCR (RT-qPCR). Cells were plated in 100-mm plates at a density of 4.0x10⁵ cells/plate in RPMI media supplemented with 10% FBS and

1% penicillin/streptomycin (pen/strep). The following day, cells were treated with either vehicle (DMSO, final concentration 0.1%), ENZ (10 μ M) or ADA-308 (concentrations of 1, 2, 5, 7.5 or 10 μ M; final concentration in 10 ml). After 72 h of treatment, the cells were washed with 1X PBS and detached in PBS/5 mM EDTA/sodium vanadate, pelleted (centrifuged at 1,200 x g for 5 min at 4°C) and resuspended in TRIzol (Thermo Fisher Scientific, Inc.; cat. no. 15596026) for RNA extraction. For reverse transcription, cDNA synthesis was performed using SuperScript™ IV Reverse Transcriptase (SSIV RT; Thermo Fisher Scientific, Inc.; cat. no. 18090010), according to the manufacturer's protocol. Briefly, 0.2 μ g RNA was mixed with oligo(dT)20 primers (Invitrogen; Thermo Fisher Scientific, Inc.; cat. no. 18418020) and dNTPs (Invitrogen; Thermo Fisher Scientific, Inc. cat. no. 10297018), and the mixture was incubated at 65°C for 5 min. After chilling on ice, the buffer, DTT and SuperScript IV enzyme were added. The reaction was carried out at 23°C for 10 min, followed by 50°C for 30 min, and terminated at 80°C for 10 min. cDNA was then used for qPCR analysis using SYBR™ Green PCR Master Mix (Thermo Fisher Scientific, Inc.; cat. no. 4309155), according to the manufacturer's instructions. Primers and cDNA templates were added to 386-well plates in triplicate. The expression of each gene was normalized to the expression of GAPDH and the $2^{-\Delta\Delta C_q}$ method (29) was used to quantify the change in expression from vehicle (DMSO) treatment. Experiments were repeated twice and the mean \pm SEM of the independent experiments are shown. The primer sequences were as follows: GAPDH forward, GGAGCGAGATCCCTC CAAAT; GAPDH reverse, GGCTGTTGTCATACTTCT CATGG; PSA/kallikrein-3 (KLK3) forward, CACAGCCTG TTTCATCCTGA; KLK3 reverse, AGGTCCATGACCTTC ACAG; homeobox protein Nkx-3.1 (NKX3.1) forward, GGA CTGAGTGAGCCTTTTGC; NKX3.1 reverse, CAGCCA GATTCTCCTTTGC; FK506 binding protein 5 (FKBP5) forward, TCCCTCGAATGCAACTCTCT; FKBP5 reverse, GCCACATCTCTGCAGTCAAA; transmembrane protease, serine 2 (TMPRSS2) forward, TGGTAGTGTCCTCCAG CCTAC; TMPRSS2 reverse, AAAGCAGCTGAAATAGGC CA; AR forward, TACCAGCTCACCAAGCTCCT; and AR reverse, GCTTCACTGGGTGTGGAAAT. The temperature protocol used for the qPCR reaction was as follows: Initial Denaturation at 95°C for 10 min; amplification cycles (35 cycles): Denaturation at 95°C for 15 sec, annealing at 60°C for 30 sec and extension at 72°C for 30 sec; final extension at 72°C for 5 min.

Microscopy. Cells were plated in RPMI media supplemented with 5% charcoal-stripped serum (Thermo Fisher Scientific, Inc.; cat. no. A3382101) on poly-L-lysine-coated coverslips at a density of 1×10^5 cells/well. The following day, the cells were pretreated with ENZ (10 μ M), ADA-308 (10 μ M) or DMSO (0.1%) for 24 h. Then, the cells were treated with either DMSO or the AR agonist, R1881, at a concentration of 10 nM for 20 min. The cells were fixed with 100% ice-cold methanol for 10 min, followed by 1X PBS washes. The cells were then incubated with anti-AR antibody (1:1,000; clone 441; Santa Cruz Biotechnology, Inc.; cat. no. sc-7305) for 1.5 h at room temperature, followed by washes with 1X PBS to remove unbound antibodies. Next, the cells were

incubated with a secondary anti-mouse Alexa 488-conjugated antibody (1:1,000; Invitrogen; Thermo Fisher Scientific, Inc.; cat. no. A21202) for 45 min at room temperature. The cells were washed with 1X PBS to remove unbound secondary antibodies, then DAPI (Thermo Fisher Scientific, Inc.; cat. no. D1306) coverslips were mounted on slides to stain the nucleus. Fluorescent images were collected using a x60 oil immersion objective, FV3000RS confocal microscope equipment and Olympus FV31S-SW software (version 2.3.2.169; Olympus Corporation).

Cell proliferation. Cells were seeded at a density of 2,000 cells per well in 96-well plates in RPMI-1640 media supplemented with 5% FBS and treated with either vehicle [DMSO (0.1%)], ENZ (10 μ M), ADA-308 (10 μ M) or ODM-201 (10 μ M). Each treatment condition was set up in 8 wells. The plates were placed in the IncuCyte live-cell analysis system (Essen Bioscience), and images were acquired every 12 h for 7 days. IncuCyte software (v2020C; Essen Bioscience) was used to analyze the cell confluency automatically over time.

Cell cycle. Cells were plated in 100-mm plates at a density of 2×10^5 cells/plate in RPMI media supplemented with 10% FBS and 1% pen/strep. The following day, the cells were treated with either vehicle (DMSO at 0.1%), ENZ (10 μ M) or ADA-380 (concentrations of 1, 2, 5, 7.5 or 10 μ M; final concentration in 10 ml). After 72 h of treatment, the cells were washed with 1X PBS and detached in PBS/5 mM EDTA/sodium vanadate, pelleted by centrifuging at 1,200 x g for 5 min at 4°C, fixed and permeabilized in 70% ice-cold ethanol for 30 min and then stored at -30°C for a minimum of 24 h. The cells were pelleted by centrifuging at 1,200 x g for 10 min at 4°C and washed in PBS, then stained in propidium iodide (PI; MilliporeSigma; cat no. P4864) solution (50 μ g/ml PI, 0.1 mg/ml RNase, 0.05% Triton X-100, 1X PBS) for 40 min at 37°C. Finally, the cells were washed and strained before flow cytometry analysis. Data were acquired by FACS on a Canti II (BD Biosciences). Data were analyzed using FlowJo software (version 10.4.2; FlowJo LLC). Representative histograms are shown in Fig. S2.

Luciferase assay. Cells were seeded in 12-well plates at a density of 1×10^5 cells/well in RPMI media supplemented with 10% FBS and 1% pen/strep. The following day, the cells were transfected with 0.2 μ g of the probasin RR3 luciferase reporter using TransIT-2020 (Mirus Bio, LLC) in Opti-MEM media (Gibco; Thermo Fisher Scientific, Inc.) following the manufacturer's protocol. The Probasin ARR3 tk-luc reporter was kindly provided by Dr Martin Gleave's Lab at Vancouver Prostate Centre (Vancouver, Canada) (30). After 24 h, the Opti-MEM transfection mix was removed and replaced with 10 μ M (final) of the compound (ENZ, ODM-201 or ADA-308) in RPMI media supplemented with 10% FBS and 1% pen/strep in triplicate. The following day, the wells were washed once with pre-warmed 1X PBS, then incubated with 200 μ l of 1X Passive lysis buffer (Promega Corporation; supplier no. E1941; cat. no. PAE1941) at room temperature with shaking for 30 min and frozen at -80°C for 45 min. The plates were thawed, the lysate was collected in microcentrifuge tubes and the debris was cleared via centrifugation at 1,200 x g for 10 min at 4°C. Next, 50 μ l (per well) of the supernatant was

added to 96-well white, flat bottom plates, then 75 μ l luciferase assay buffer (Promega Corporation; cat. no. E1910) was automatically injected per well. After 30 sec of incubation, signal was detected by a luminescent plate reader (Tecan infinite M200Pro). Fluorescence units were normalized to the protein concentration per sample (BCA assay) and calculated relative to the control condition [DMSO for LNCaP; ENZ (10 μ M) for 49C^{ENZ}R and 49F^{ENZ}R]. Experiments were repeated three times, and the mean \pm SEM of the independent experiments was calculated.

RNA-sequencing (RNA-seq). Cells were grown in RPMI-1640 media supplemented with 5% FBS and DMSO (0.1%), ENZ (10 μ M) or ADA-308 (10 μ M). Total RNA was isolated from the cells after 72 h of treatment using the PureLink RNA Mini Kit (Thermo Fisher Scientific, Inc.). The library was generated using the NEBnext Ultra ii Stranded RNA Library Prep Kit (New England BioLabs, Inc.; cat. E7770S), the quality of the RNA samples was assessed by measuring the 230/260 and 260/280 ratio using a NanoDrop spectrophotometer (Thermo Fisher Scientific, Inc.), ensuring values were >1.8 and 2, respectively. Sequencing was performed on an Illumina NextSeq 500 (42x42-bp paired-end reads) by the University of British Columbia Sequencing + Bioinformatics Consortium (Vancouver, Canada), targeting 20 million reads per sample. Data was de-multiplexed using bcl2fastq2 Conversion Software (version 2.20; Illumina, Inc.), and read sequences were aligned to the human reference genome, hg38, using STAR aligner (version 2.7.8a) (31). Assembly and differential expression were estimated using Cufflinks software (version 2.2.1) (32), available through the Illumina BaseSpace Sequence Hub. Gene expression data (raw count data) were normalized using 'DESeq' (33) in Rstudio (version 4.1.2; <https://cran.r-project.org/>), and subsequently, log2 was transformed. Unsupervised clustering was generated using R, and data were visualized using the R 'ggplot' program or GraphPad Prism (version 8; Dotmatics). The significance of the expression level differences between the treatment samples was determined using an unpaired t-test in GraphPad Prism or R.

Chromatin immunoprecipitation-sequencing (ChIP-seq) data analysis. ChIP-seq Fastq files were downloaded from the Gene Expression Omnibus (<https://www.ncbi.nlm.nih.gov/geo/>). Publicly available AR ChIP-seq datasets [GSM1069669 and GSM1236925, from Chen *et al* (34)] used in the present study from were downloaded from GSE43791. Publicly available control LNCaP RNA-seq [GSM4777223 and GSM4777224, from Davies *et al* (26)] data were downloaded from GSE138460. Data was processed using FastQC (version 0.11.9) (35) for quality control analysis. Adapter sequences were removed using Cutadapt (version 1.18; <https://cutadapt.readthedocs.io/en/stable/>) and reads were aligned to the human genome reference, hg38, using BWA-MEM software (version 0.7.17) (36). SAM files were converted to BAM files using SAMtools software (version 1.1.2) (37). MACS2 (version 2.2.7.1) (38) was used to call peaks with a false discovery rate (FDR) of 0.05 using the narrow peak caller for AR-bound genes. DeepTools (version 2.30.0) (39) was used to visualize data, and BEDtools (version 2.28.0) (40) generated shared and unique peaks between dihydrotestosterone (DHT) and ENZ AR

ChIP-seq samples. The peaks were annotated using HOMER (version 3.0; <http://homer.ucsd.edu/homer/>).

Gene ontology and pathway analysis. Pathway analysis was conducted using gene set enrichment analysis (GSEA) software, available from the Broad Institute (Massachusetts Institute of Technology) and gProfiler (41). This analysis aimed to discern the functions associated with differentially expressed genes within the Molecular Signatures Database (version 7.1) (42). The GSEA tool was utilized in classic mode to identify significantly enriched biological pathways. Pathways exhibiting enrichment with a nominal $P < 0.05$ and FDR < 0.25 were considered statistically significant. For single-sample GSEA, gProfiler, a web server designed for functional enrichment analysis and the conversion of gene lists, was utilized.

Statistical analysis. Statistical analysis was conducted using Microsoft Excel and GraphPad Prism software (version 8; Dotmatics). All presented *in vitro* experiments were independently replicated a minimum of three times. To analyze data variance between multiple groups, a one-way ANOVA followed by the Dunnet's test were used to perform multiple comparisons within each group compared with the control group, which is depicted in bar charts. For longitudinal profiling experiments, a two-tailed unpaired Student's t-test was performed to determine the statistical difference at the final time point. Visualization was performed using GraphPad Prism 8 or Rstudio (version 4.1.2; <https://cran.r-project.org/>). $P < 0.05$ was considered to indicate a statistically significant difference.

Results

Introduction to ADA-308. ADA-308, a novel arylamide compound, emerged following an extensive and meticulous design process involving the synthesis and evaluation of over 650 carefully crafted structures, comprising >220 profiled small molecules and various chemical scaffolds. In preliminary pharmacokinetic studies (unpublished data), ADA-308 exhibited notable characteristics in mice. When administered orally at 100 mg/kg in mice, ADA-308 displayed a plasma half-life ($T_{1/2}$) of 10.9 h. In comparison, oral administration of ADA-308 at a 30 mg/kg dose in rats resulted in a plasma $T_{1/2}$ of 12.6 h. ADA-308 was designed to address treatment resistance observed with other AR antagonists. The compound was designed considering optimized binding affinity to the AR, improved pharmacokinetic properties and its ability to retain AR antagonism in CRPC cells (such as when AR is upregulated or mutated). In addition to ENZ-resistant conditions (such as F876L AR mutation), ADA-308 was screened in a panel of CRPC AR mutants (T877A and W741L), where it retained its antagonistic activity, highlighting its potential as a versatile and practical treatment option.

ADA-308 suppresses AR transcriptional activity in Adeno and ENZ-resistant cell lines. To assess the impact of ADA-308 treatment on AR signalling, the prostate Adeno cell line, LNCaP, was treated with ADA-308. A dose-dependent decrease in the expression of PSA, a canonical AR target, was observed, which was similar to that observed following ENZ

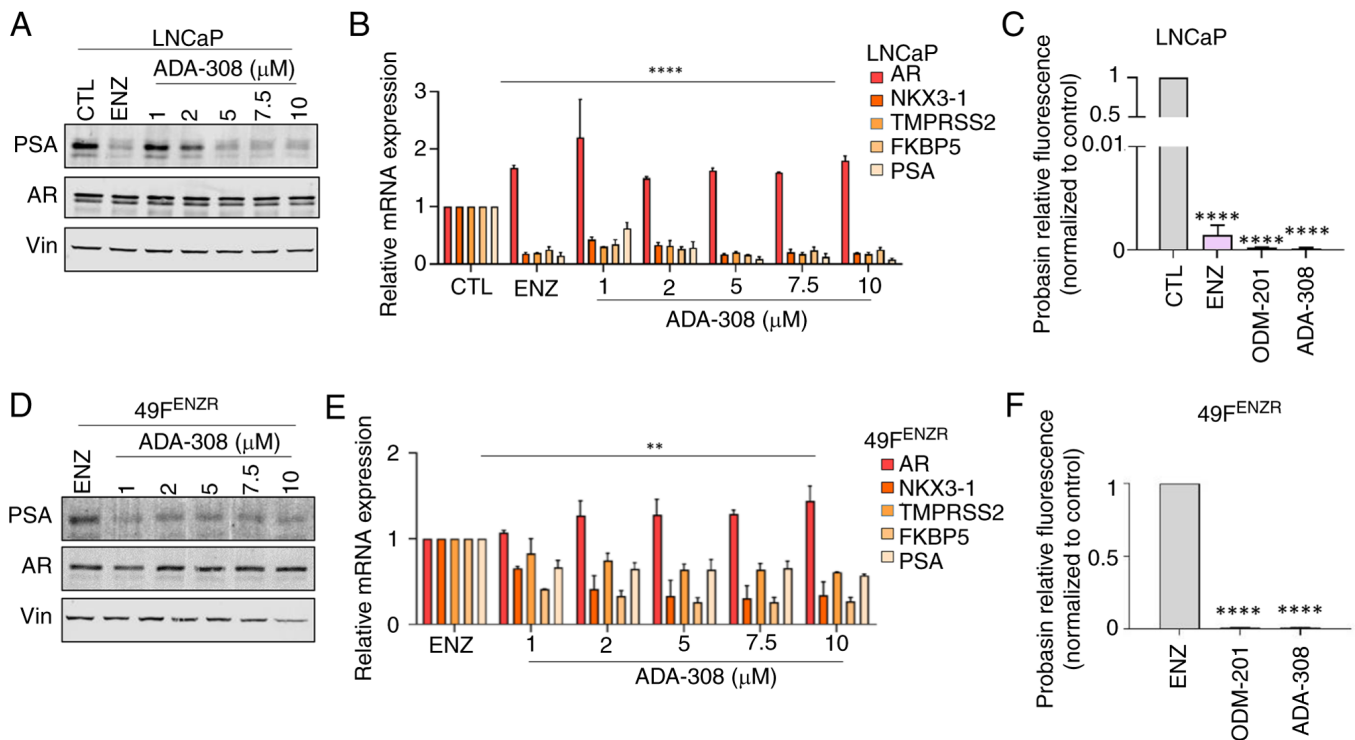


Figure 1. ADA-308 decreases AR activity in adenocarcinoma and ENZ-resistant prostate cancer cell lines. (A) Western blot shows that treatment with ADA-308 inhibited PSA (canonical AR target) expression in ENZ-sensitive LNCaP cells in a dose-dependent manner (1-10 μ M). ENZ (10 μ M) was used as a positive CTL. Cells were treated for 72 h before protein lysate was harvested (n=3 independent biological replicates). Vin was used as the loading CTL. (B) ADA-308 decreased the transcription of AR target genes in the LNCaP cell line, as shown by RT-qPCR. Cells were treated for 72 h with 10 μ M ENZ or 1-10 μ M ADA-308 before RNA was extracted (n=3 independent biological replicates). (C) ADA-308 at 10 μ M inhibited AR transactivation, as measured by luciferase assay with R1881-induced activation of probasin AR reporter in LNCaP cells (n=2 independent biological replicates). Data shows relative fluorescence normalized to the CTL (DMSO). (D) Western blot shows that treatment with ADA-308 inhibited PSA expression in ENZ-resistant 49F^{ENZ}R cells in a dose-dependent manner (1-10 μ M). ENZ (10 μ M) was used as the CTL. Cells were treated for 72 h before protein lysate was harvested (n=3 independent biological replicates). Vin was used as the loading CTL. (E) ADA-308 decreased the transcription of AR target genes in the 49F^{ENZ}R cell line as shown by RT-qPCR. Cells were treated for 72 h with 1-10 μ M ADA-308 or 10 μ M ENZ before RNA was extracted (n=2 independent biological replicates). (F) ADA-308 at 10 μ M inhibited AR transactivation, as measured by luciferase assay with R1881-induced activation of probasin AR reporter in 49F^{ENZ}R cells. Data shows relative fluorescence normalized to ENZ (n=2 independent biological replicates). All data were analyzed using a one-way ANOVA to assess the variance between dosages. Post hoc comparisons were performed using Dunnett's test to compare each treatment group to the control. Data are presented as the mean \pm standard deviation. **P<0.01, ****P<0.0001. All exact P-values are listed in Table SI. 49F^{ENZ}R, 49F ENZ-resistant; AR, androgen receptor; CTL, control; ENZ, enzalutamide; PSA, prostate-specific antigen; RT-qPCR, reverse transcription-quantitative PCR; Vin, vinculin.

treatment (Fig. 1A). The mRNA expression of other canonical AR targets also decreased in a dose-dependent manner, comparable to ENZ (Fig. 1B and Table SI). Furthermore, using an androgen-responsive luciferase reporter linked to the probasin (43) promoter, known for its robust AR-specific and tissue-specific regulation (43), it was observed that ADA-308 significantly and efficiently reduced AR activity. This was similar to the results achieved with ENZ or ODM-201 (high-affinity AR antagonists) (27) (Fig. 1C).

CRPC is often treated with the potent AR antagonist, ENZ, which frequently leads to ENZ resistance through the re-activation of the AR signalling axis. To model ENZ-resistant disease, with re-activation of AR signalling, our lab previously generated ENZ-resistant cell lines, 49C^{ENZ}R and 49F^{ENZ}R, by serially passaging the PCa Adeno cell line, LNCaP, in castrated mice treated with ENZ (28). These cell lines are derived from PSA⁺ tumors and retain PSA expression (44). These cell lines harbour the AR F876L activating mutation (45), a rare mutation in the early stages of the disease that is frequently observed in CRPC (46) and ENZ-resistant tumors (47,48). By altering the ligand binding pocket of AR, F876L allows other steroid hormones (such as corticosteroids

and anti-androgens) to activate AR (49), rendering ENZ an agonist that drives phenotypic resistance (47,48). To explore the potential of re-targeting AR signaling in these models, the effect of ADA-308 on AR-dependent genes was investigated. The findings revealed that treatment with ADA-308 exhibited a dose-dependent reduction in PSA expression in both 49C^{ENZ}R and 49F^{ENZ}R (Figs. 1D and S3A). This reduction in AR activity was reflected by decreased mRNA expression of canonical AR target genes (Figs. 1E, S3B, and Table SI) and a significant decrease in probasin luciferase activity (Figs. 1F and S3C). Notably, treatment of LNCaP with either ENZ, ADA-308 or ODM-201 resulted in a reduction in the PSA mRNA level (Fig. S3D), with no differences observed between the different compounds. Taken together, these data demonstrated that ADA-308 acts as an AR signaling inhibitor in Adeno, particularly in ENZ-resistant cell line models.

ADA-308 inhibits AR nuclear localization in Adeno and ENZ-resistant cell lines. AR, a nuclear transcription factor that belong to the steroid hormone receptor superfamily (50), is activated upon binding of androgens (51). In the absence of a ligand, AR primarily resides in the cytoplasm and often form

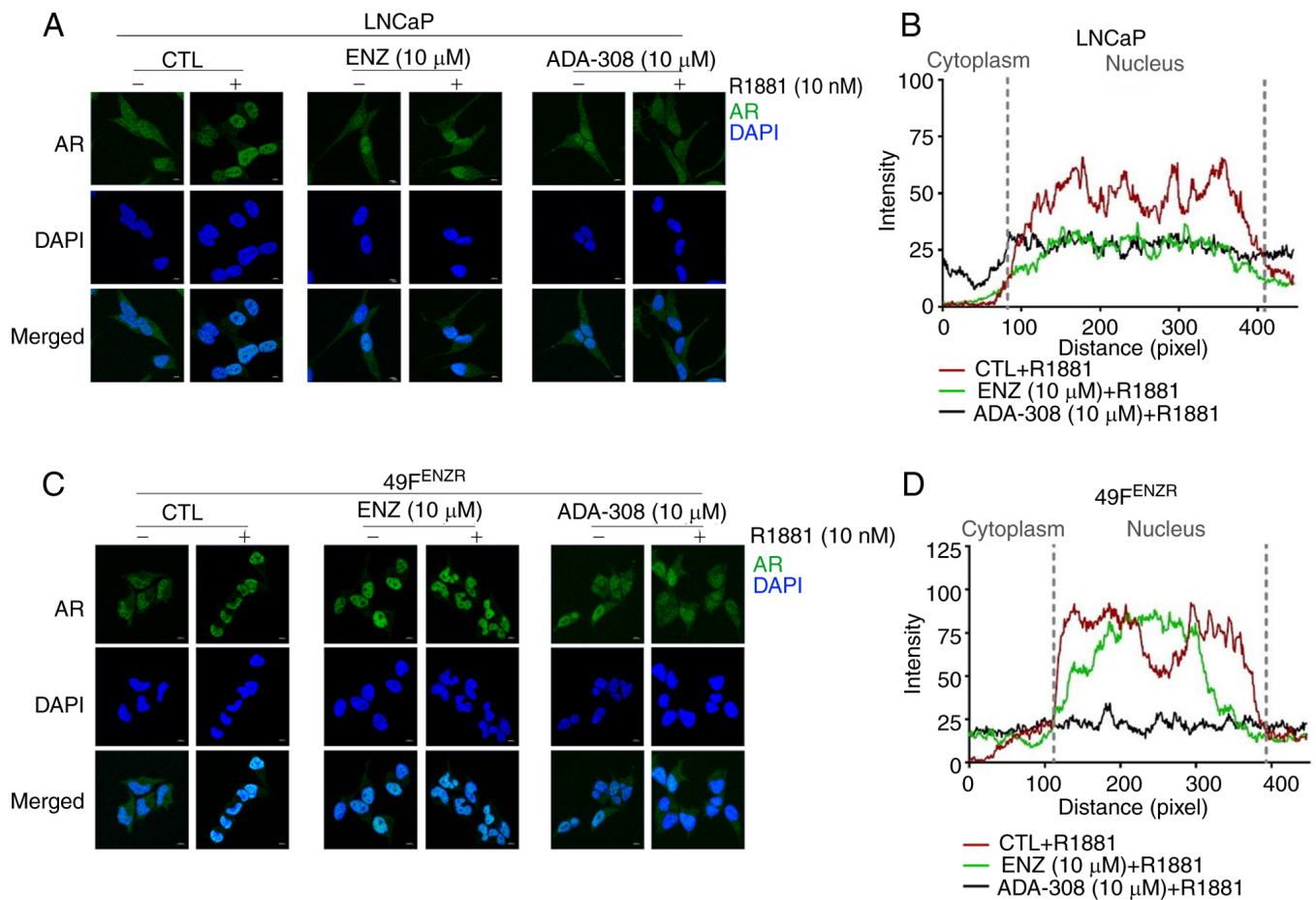


Figure 2. ADA-308 inhibits AR nuclear translocation in adenocarcinoma and ENZ-resistant prostate cancer cell lines. (A) Immunofluorescence of LNCaP treated with DMSO (CTL), AR antagonists ENZ (10 μM) or ADA-308 (10 μM) for 24 h with or without a 20-min R1881 (10 nM) treatment; scale bar, 10 μm. AR is shown in green and DAPI in blue. (B) Co-localization of AR and the nuclei of LNCaP cells in the immunofluorescence data, as measured by Zen software. Data are shown as DMSO (red), ENZ (green) and ADA-308 (navy) plus R1881. (C) Immunofluorescence of 49F^{ENZ}R cells treated with DMSO (CTL), AR antagonists ENZ (10 μM) or ADA-308 (10 μM) for 24 h with or without a 20-min R1881 (10 nM) treatment; scale bar, 10 μm. AR is shown in green and DAPI in blue. (D) Co-localization of AR and nuclei in 49F^{ENZ}R cells in the immunofluorescence data, as measured by Zen software. Data are shown as DMSO (red), ENZ (green) and ADA-308 (navy) plus R1881. 49F^{ENZ}R, 49F ENZ-resistant; AR, androgen receptor; CTL, control; ENZ, enzalutamide.

complexes with heat shock protein chaperones (52). However, in the presence of ligands, AR undergo homodimerization, translocates to the nucleus and attaches to androgen response elements to initiate transcription (53).

Notably, in the Adeno cell line, LNCaP, and the ENZ-resistant cell lines, 49C^{ENZ}R and 49F^{ENZ}R, AR was predominantly localized to the cytoplasm. However, AR translocates to the nucleus upon stimulation with synthetic androgen (R1881). Immunofluorescence microscopy showed that treatment with ADA-308 inhibited AR nuclear translocation in the LNCaP cell line, similar to the effect observed for ENZ (Fig. 2A and B), suggesting that both ADA-308 and ENZ effectively hindered the androgen-induced nuclear translocation of AR. In addition, AR was observed in the cytoplasm and nucleus of the ENZ-resistant cell lines, 49C^{ENZ}R and 49F^{ENZ}R. However, treatment with R1881 increased the ratio of nuclear AR to cytoplasmic AR (Fig. 2C and D). Notably, ADA-308 treatment markedly prevented the androgen-induced nuclear translocation of AR, whereas ENZ treatment failed to do so (Figs. 2C, 2D and S4A). These results suggested that, following the development of ENZ resistance, ADA-308 exerted its inhibitory effect on AR signaling by preventing AR nuclear

translocation. These data highlight the potential of ADA-308 as an antagonist of mutated AR and warrant further investigation into its clinical response, particularly in ENZ-resistant tumors.

ADA-308 inhibits proliferation *in vitro*. Next, the anti-proliferative properties of ADA-308 and its impact on the cell cycle were assessed. A reduction in the proliferation rate of LNCaP cells was observed upon treatment with either ADA-308 or ENZ, with ADA-308 exhibiting a more pronounced suppression of cell proliferation than ENZ (Fig. 3A). Moreover, ADA-308 treatment resulted in a modest increase in G0/G1 arrest; a ~9% increase in the G0/G1 cell population was observed, which was comparable to the ~8% increase following ENZ treatment (Figs. 3C and S4). Next, the effect of ADA-308 on ENZ-resistant cell lines was evaluated. Similar to the observations in the Adeno cell line, ADA-308 notably suppressed ENZ-resistant cell proliferation (Figs. 3B and S4B). However, it was observed that ODM-201 had a more profound effect on the cell proliferation (Fig. S4B). In addition, a significant increase in the G0/G1 cell population in the ENZ-resistant cells after ADA-308 treatment was observed (Figs. 3D, S4C).

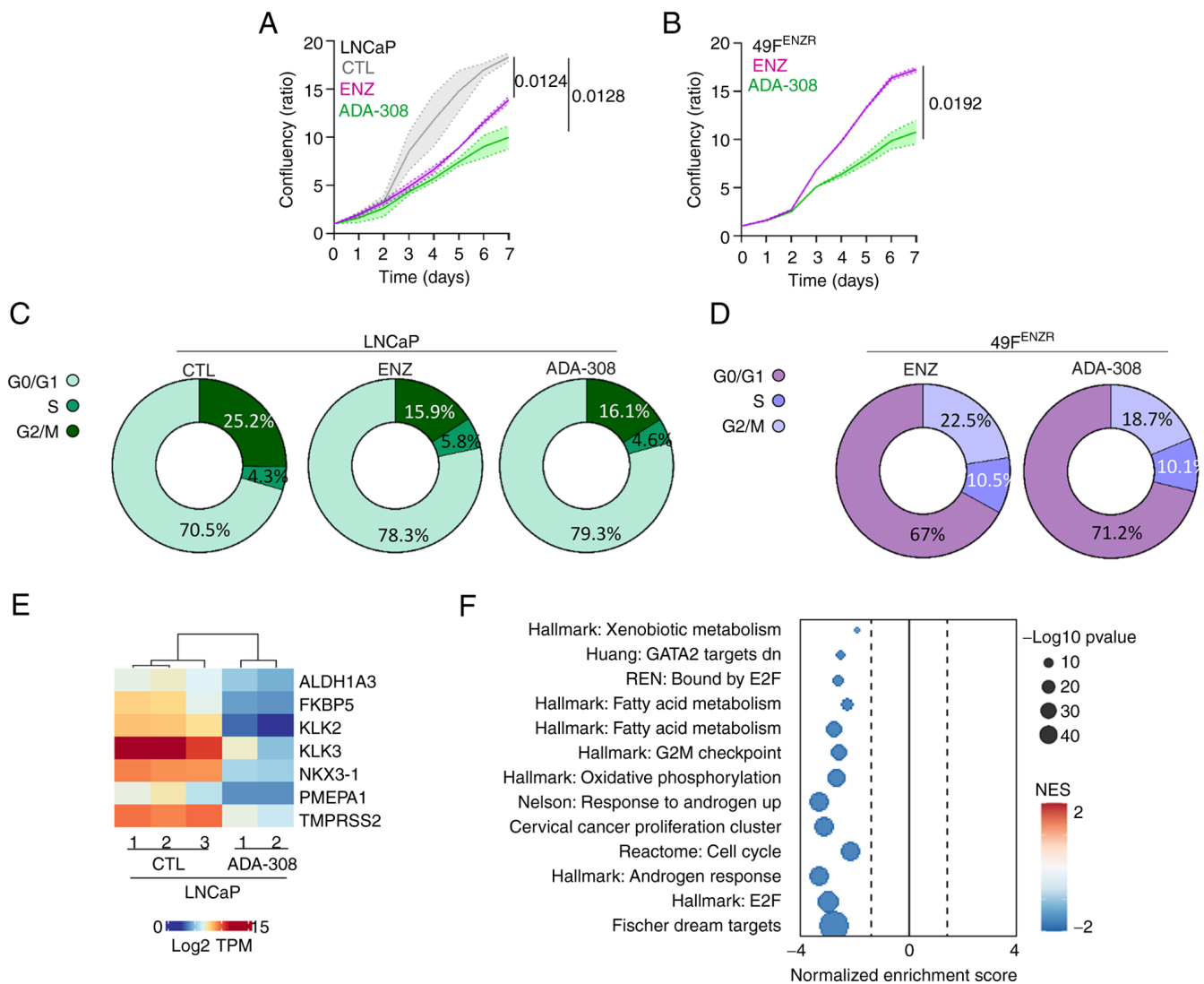


Figure 3. ADA-308 induces G1 accumulation and inhibits proliferation *in vitro*. (A) LNCaP and (B) 49F^{ENZ} cell lines were treated with DMSO, ENZ (10 μ M) or ADA-308 (10 μ M) for 7 days, and proliferation was measured using IncuCyte and reported as confluency ratio over day 0. n=3 independently biological replicates; data are presented as the mean \pm standard deviation. Significance was evaluated at the endpoint using unpaired, two-tailed Student's t-test or one-way ANOVA. Post hoc comparisons were performed using Dunnett's test to compare each treatment group to the control. (LNCaP ENZ vs. CTL, P=0.0124; LNCaP ADA-308 vs. CTL, P=0.0128; 49F^{ENZ} ADA-308 vs. ENZ, P=0.0192). (C) LNCaP and (D) 49F^{ENZ} cell lines were treated with CTL, ENZ (10 μ M) or ADA-308 (10 μ M) for 72 h, and the cell cycle was assessed using flow cytometry. Two-tailed unpaired t-test or one-way ANOVA followed by Dunnett's test was used to compare treatment to the CTL group (LNCaP ENZ vs. CTL: G0/G1, P=0.003; S, P=0.00029; G2/M, P=0.179; LNCaP ADA-308 vs. CTL: G0/G1, P=0.0002; S, P=0.0001; G2/M, P=0.319; 49F^{ENZ} ADA-308 vs. CTL: G0/G1, P=0.008; S, P=0.011; G2/M, P=0.125); n=3 independently biological replicates. See Figure S2 for the representative histograms. (E) LNCaP was treated with ADA-308 (10 μ M) for 72 h and samples were collected for RNA-sequencing. The heatmap shows the log2TPM values of canonical androgen receptor target genes. (F) Gene Set Enrichment Analysis identified pathways differentially regulated in LNCaP treated with ADA-308 (10 μ M) for 72 h compared with the CTL. 49F^{ENZ}, 49F ENZ-resistant; CTL, control; ENZ, enzalutamide; NES, normalized enrichment score; TPM, transcripts per million.

To understand the biological impact of ADA-308, LNCaP cells were treated with ADA-308 and RNA-seq was performed. First, the changes in AR signalling induced by ADA-308 treatment were assessed. A notable inhibition of AR activity was observed as evidenced by a marked reduction in the expression of canonical AR targets (Fig. 3E). GSEA was performed to identify a range of pathways altered by ADA-308 treatment. As expected, the downregulation of AR-regulated pathways following ADA-308 treatment was observed. Notably, ADA-308 significantly inhibited pathways crucial for cell proliferation and cycle progression (Fig. 3F). These observations highlighted the promising anti-proliferative properties of ADA-308 in Adeno *in vitro*, particularly in the

context of ENZ-resistance models that are resistant to existing treatments.

ADA-308 modulates AR-bound target genes and associated pathways. To evaluate the efficacy of ADA-308 in comparison with ENZ, RNA-seq of LNCaP cells treated with either ADA-308 or ENZ was conducted. Unsupervised clustering revealed that the treated samples clustered together and were distinct from those of the control group (Fig. 4A). Although a significant number of differentially expressed genes after treatment with these AR inhibitors was observed (Fig. 4B), the difference between ADA-308 and ENZ was not statistically significant (Fig. 4C). Subsequent analysis identified 1,081

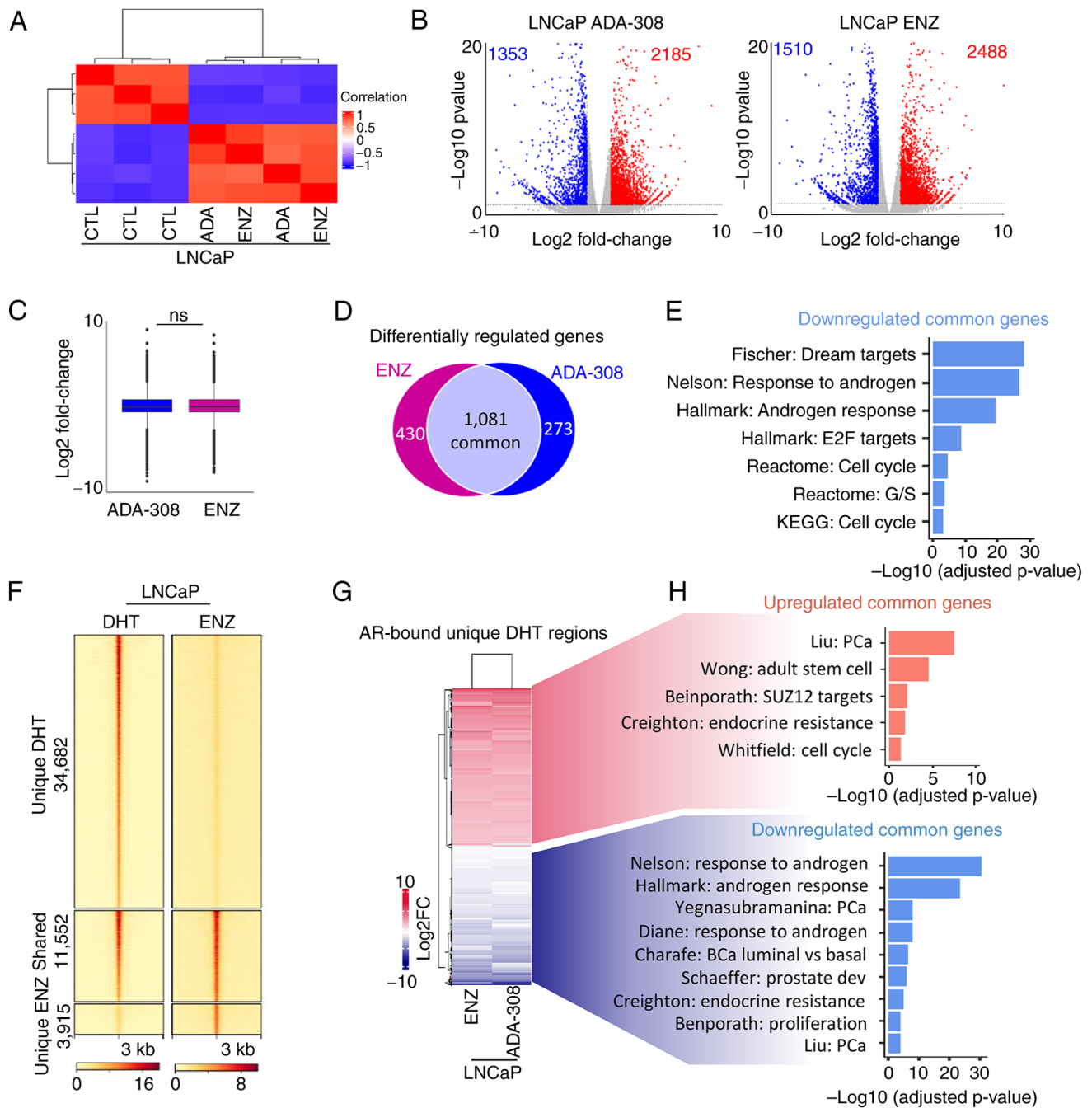


Figure 4. Effectiveness of ADA-308 is comparable to ENZ. (A) Unsupervised clustering using RNA-sequencing data from LNCaP treated with ENZ (10 μ M) or ADA-308 (10 μ M) for 72 h shows a correlation between the CTL and treatment groups. (CTL n=3 and treatment n=2 independent biological replicates). (B) Volcano plot shows genes differentially regulated after treatment with ADA-308 (10 μ M) (left) or ENZ (10 μ M) (right). Each dot represents 1 gene. Blue dots represent genes downregulated >1 log2FC with P<0.05, and red dots represent genes upregulated >1 log2FC with P<0.05. (C) The box plot shows an average expression of all differentially regulated genes following ENZ (10 μ M) or ADA-308 (10 μ M) treatment compared with the CTL, presented as log2FC. (D) Number of differentially regulated genes following ENZ (10 μ M) or ADA-308 (10 μ M) treatment compared with the CTL. Genes common between the two treatment groups are shown in the gray section, P<0.05. (E) Gene Set Enrichment Analysis was performed on commonly downregulated genes between ENZ (10 μ M) or ADA-308 (10 μ M) treatment compared with the CTL with P<0.05. Data are presented as -log10 of the adjusted P-value. (F) A heatmap of AR binding intensity in LNCaP cells treated with DHT or ENZ is presented as a fold change over input, with each horizontal line representing a 3 kb locus. Clusters are shown as regions unique to DHT treatment (regions lost AR binding after ENZ treatment), regions shared between DHT and ENZ treatment and regions unique to ENZ (regions gained AR binding after ENZ treatment). (G) Heatmap shows expression of all AR-bound annotated genes in unique DHT regions in ENZ (10 μ M) or ADA-308 (10 μ M). Presented as log2FC. (H) Pathways associated with commonly upregulated genes in ENZ (10 μ M) and ADA-308 (10 μ M). Red, common upregulated genes in ENZ and ADA-308; blue common downregulated genes in ENZ and ADA-308, using gProfiler. Data are presented as -log10 of the adjusted P-value, P<0.05. AR, androgen receptor; CTL, control; DHT, dihydrotestosterone; ENZ, enzalutamide; FC, fold change; ns, not significant.

genes that were downregulated by both ADA-308 and ENZ treatments (Fig. 4D). GSEA revealed that these commonly downregulated genes were associated with pathways regulating

the cell cycle, proliferation and the androgen response (Fig. 4E and Table SII). This was consistent with our previous findings demonstrating that ENZ treatment led to reduced proliferation

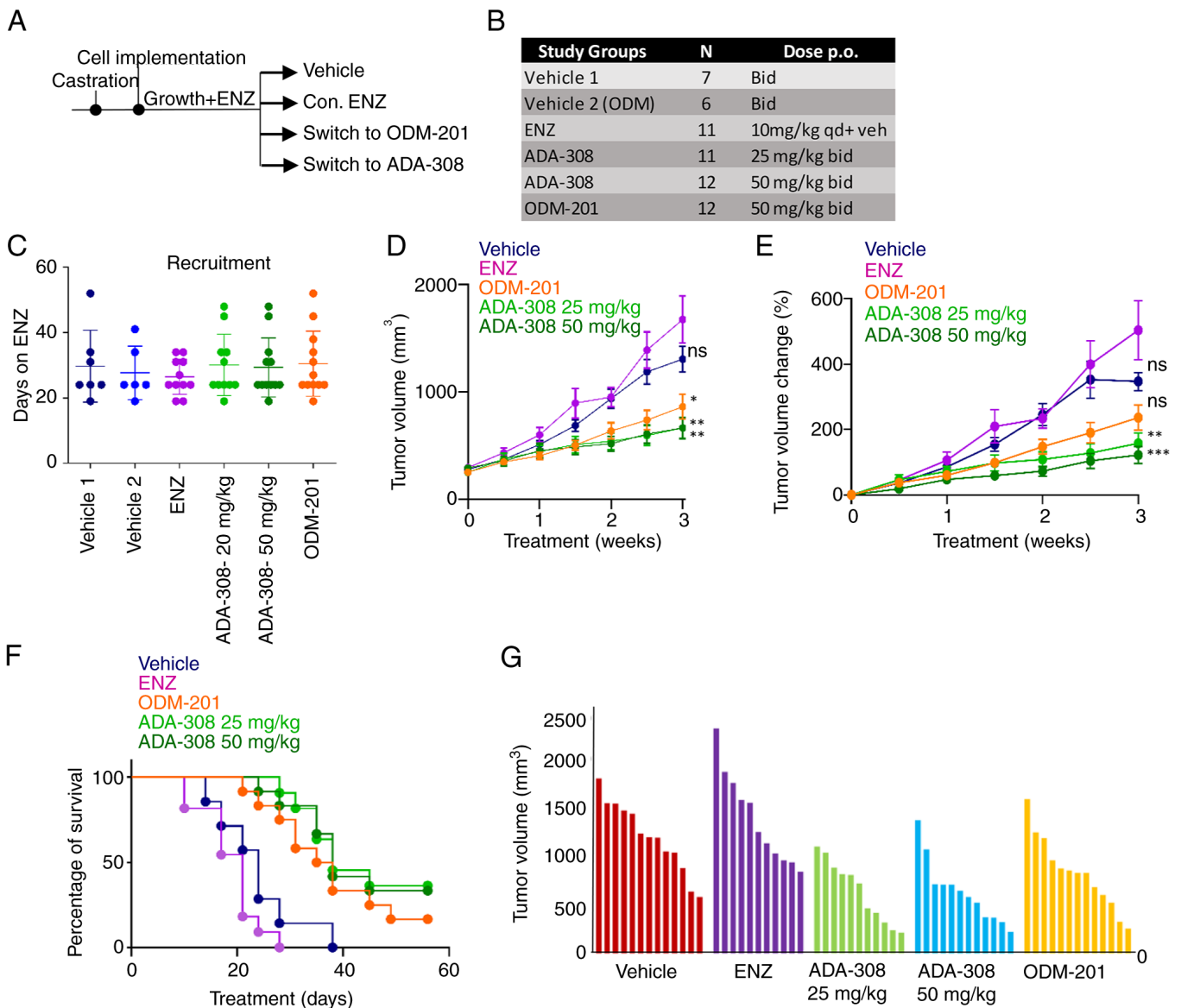


Figure 5. ADA-308 reduces serum PSA and tumour growth in ENZ-resistant cells *in vivo*. (A) Schematic of the *in vivo* study. (B) *In vivo* study treatment groups, number of mice recruited to each group and the respective doses. (C) *In vivo* recruitment details are shown as days on ENZ before recruitment to the respective treatment group. Castrated Nu/Nu mice were inoculated with bilateral 49P^{ENZ} tumors, and tumor dimensions were measured biweekly. Mice were assigned to vehicle group 1, vehicle group 2, continuum on ENZ (10 mg/kg), two doses of ADA-308 (25 mg/kg and 50 mg/kg) or ODM-201 (50 mg/kg). (D) Tumor volume shown as mm³ (P-values were calculated at the endpoint, comparing ENZ with the vehicle: 0.0307; ODM-201 with the vehicle: 0.0369; ADA-308 25 mg/kg with the vehicle: 0.0335; ADA-308 50 mg/kg with the vehicle: 0.0302. P-values were calculated using one-way ANOVA statistical test followed by Dunnett's test). (E) Tumor volume change presented as a percentage over 3 weeks of treatment. (P-value was calculated at the endpoint, comparing ENZ with the vehicle: 0.2665; ODM-201 with the vehicle: 0.0261; ADA-308 25 mg/kg with the vehicle: 0.0118; ADA-308 50 mg/kg with the vehicle: 0.0144. P-values were calculated using one-way ANOVA statistical test followed by Dunnett's test). (F) Cancer-specific survival indicates the percentage of mice with a tumour size <1,500 mm³ at a given treatment day. (G) Tumor volume (mm³) for the individual mice in each treatment group after 3 weeks of treatment. Vehicle groups 1 and 2 are combined. *P<0.05, **P<0.01, ***P<0.001. See Table SI for the statistical test results. Bid, twice a day; ENZ, enzalutamide; ns, not significant; PSA, prostate-specific antigen; qd, four times a day.

and induced G0/G1 arrest in LNCaP cell lines (54,55), but notably highlighting the effectiveness of ADA-308 in the context of ENZ-resistant models where ENZ was less responsive (Fig. 3A-D).

To delve deeper, publicly available AR ChIP-seq data were leveraged (34). The regions bound by the AR in the presence of DHT or ENZ were examined. Notably, a substantial number of AR-bound regions (34,682 peaks) were lost following ENZ treatment (Fig. 4F), consistent with previous reports indicating that ENZ reduces AR chromatin binding and nuclear localization (56) and in alignment with aforementioned

observations (Fig. 2A and B). However, despite ENZ treatment, ~15,000 regions remained bound by AR. The AR-bound regions that were lost following ENZ treatment were specifically focused on, and 12,382 genes within this region were identified (Fig. 4F). Following integration of the RNA-seq data, a significant association between ADA-308 and ENZ-regulated AR target genes was revealed (Fig. 4G). Moreover, the GSEA results shed light on the functional consequences of these alterations, with AR-bound genes upregulated following treatment associated with stemness, whereas downregulated genes were linked to androgen signaling, luminal phenotype

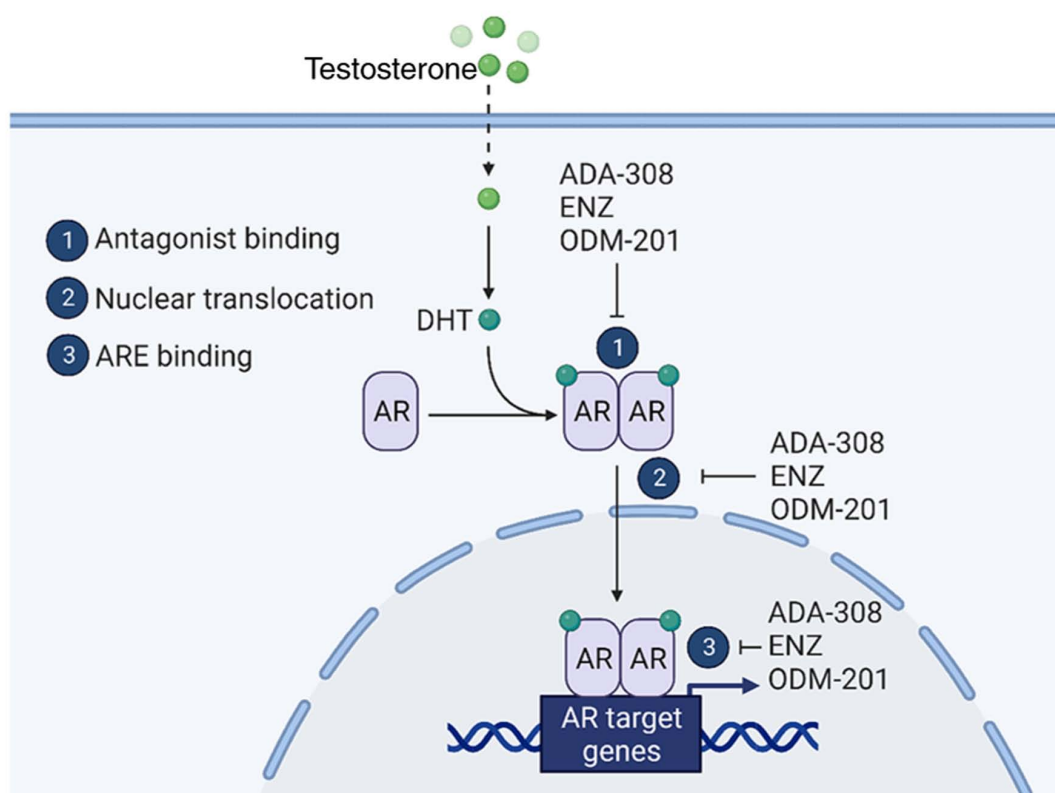


Figure 6. Schematic of the ADA-308 mechanism of action. Created using BioRender.com. AR, androgen receptor; ARE, AR element; DHT, dihydrotestosterone; ENZ, enzalutamide.

and proliferation (Fig. 4H). Collectively, these data suggested that ADA-308 exerted effects comparable to those of ENZ in modulating critical AR-bound target genes and their associated pathways.

ADA-308 reduces tumor growth *in vivo*. Investigation into the effects of ADA-308 revealed its ability to inhibit cell proliferation *in vitro*. To assess the *in vivo* pharmacodynamics activity of ADA-308, castrated mice harboring 49F^{ENZ} ENZ-resistant xenograft tumors were treated with ADA-308, ENZ or ODM-201 for comparison. For this, male athymic mice were castrated and allowed to recover from surgery. Then, ENZ-resistant 49F^{ENZ} cells were inoculated, and mice were administered ENZ daily until the tumor volume reached 200 mm³. Thereafter, the treatment regimens were adjusted, with ENZ either continued or replaced with vehicle, ADA-308 at 25 mg/kg BID, ADA-308 at 50 mg/kg BID or ODM-201 at 50 mg/kg BID (Fig. 5A-C and Table SIII). The mice were treated for up to 8 weeks or until the tumor volume reached 1,500 mm³.

The reduction in proliferation rates observed *in vitro* translated into a notable *in vivo* antitumor response. It was observed that both doses of ADA-308 (25 or 50 mg/kg) exhibited improved antitumor responses in the ENZ-resistant cell model compared with ENZ or ODM-201. Notably, in the ENZ-treated group, most mice reached the study endpoint by 3 weeks (Fig. 5D). The percentage change in tumor volume after treatment with ADA-308 was significantly lower (Fig. 5E and Table SIV), leading to higher survival rates (Fig. 5F and Table SIII). Notably, prior ENZ administration did not

compromise the efficacy of ADA-308. In addition, testing lower doses of ADA-308 (12.5 mg/kg BID) resulted in a significantly reduced tumor volume in ENZ-resistant tumors (Fig. S5A-C). Overall, these data elucidated the *in vivo* efficacy of ADA-308 and its superior capacity to inhibit tumor growth in ENZ-resistant 49F^{ENZ} xenograft models.

Discussion

It is now understood that CRPC retains its androgen sensitivity, both in the early stages of the disease as well as following the successful treatment with next-generation ARPIs (9,57,58). This dependence on the AR for growth (59-61) highlights the continued significance of the AR as a therapeutic target in PCa (62). However, the response to second-generation ARPIs is often only temporary, and resistance poses an unavoidable challenge. As a result, several AR antagonists including ARN-509 (47) and ODM-201 (27), have been developed and evaluated for inhibition of AR activity. Therefore, development of alternative and novel AR-targeted therapies is of paramount importance.

The ADA-308 compound was originally designed to overcome the treatment resistance to other AR antagonists in advanced PCa. The present study demonstrated that ADA-308 can potentially reduce AR activity in ENZ-sensitive and ENZ-resistant preclinical models. The investigation encompassed two distinct PCa cell models: LNCaP (representing Adeno) and the ENZ-resistant 49F^{ENZ} and 49C^{ENZ} cell lines (which no longer responded to ENZ treatment). Administration of ADA-308 in these models resulted in a significant inhibition

of AR signalling and the accumulation of cells in the G0/G1 phase of the cell cycle, a response comparable to that of ENZ in LNCaP cells. It was therefore demonstrated that ADA-308 is a very potent AR inhibitor in PCa research models including those resistant to ENZ. Mechanistically, it was shown that the mechanism of action of ADA-308 closely parallels that of ENZ and ODM-201 (Fig. 6). Notably, ADA-308 hindered androgen-induced AR nuclear localization in LNCaP cells, which is a critical step in AR activation and targeted gene transcription. In ENZ-resistant (49F^{ENZ^R} and 49C^{ENZ^R}) cell lines, ENZ significantly failed to inhibit androgen-induced AR nuclear localization, while ADA-308 prevented this effect. Moreover, comparing the effect of ADA-308 to ENZ on the transcriptome of LNCaP cells, the data revealed that ADA-308 was comparable to ENZ in suppressing genes regulated by the AR or those associated with proliferation. Notably, upon ADA-308 treatment of LNCaP cells, an increased expression of AR-bound genes associated with the stemness pathway was observed, similar to ENZ treatment. This raises a noteworthy concern regarding whether treatment with ADA-308 can induce lineage plasticity. Lineage plasticity has been postulated to contribute to the failure of ARPIs in PCa, representing an established mechanism of treatment resistance associated with the loss of luminal lineage, and an induction of alternative programs including stem cell-like phenotypes (26,63-65). Therefore, it is important to evaluate whether ADA-308 induces lineage plasticity.

In the present study, ADA-308 demonstrated a superior *in vitro* anti-proliferative effect compared with ENZ in ENZ-resistant cell line models. Moreover, the presented *in vivo* study provided compelling evidence that ADA-308 reduced tumor growth in ENZ-resistant models. The anti-tumor effect of ADA-308 was accompanied by an increase in overall survival. Collectively, these findings suggested that ADA-308 may emerge as a promising and viable candidate for future clinical development in CRPC, particularly in an ENZ-resistant context where ENZ treatment has failed, thereby offering a viable treatment strategy in the evolving landscape of PCa therapy. Finally, a more comprehensive understanding of the safety profile, long-term effects and potential resistance mechanisms of ADA-308 is essential as we consider its transition into clinical development.

Although the present study provided valuable insights into the therapeutic potential of ADA-308 in PCa, particularly in overcoming resistance to other AR antagonists such as ENZ, there are some limitations to the findings. One limitation of the present study is the limited number of models, which may not fully represent the genetic and phenotypic diversity of PCa observed in a broader patient population. Additionally, the *in vivo* studies were conducted exclusively in mouse models, which, despite their utility, cannot perfectly mimic the complex human tumor micro-environment and immune interactions. Notably, ARPIs can lead to the development of lineage plasticity, a mechanism of resistance in which cells alter their lineage to acquire an alternative lineage that is often associated with stem-cell and neuronal characteristics. Therefore, future studies are needed to better characterize whether ADA-308 treatment leads to the activation of resistance mechanisms, including lineage plasticity. Additionally, longitudinal studies

monitoring long-term outcomes and potential side effects are essential to ensure that ADA-308 can provide sustainable benefits for the treatment of PCa. In addition, while it was shown that ADA-308 reduced PSA expression similar to ODM-201 and that the *in vivo* effects of the compounds were similar, without further investigation regarding the long-term effect of ADA-308, we cannot comment on whether ADA-308 will be a preferred option for treatment of PCa to ODM-201.

In the present study, the significant efficacy of ADA-308 in suppressing AR signalling and reducing proliferation *in vitro* and *in vivo* was highlighted. These findings are particularly noteworthy and relevant given the growing occurrence of resistance to potent ARPIs (66-68) and the limited number of therapeutic options following the development of resistance. The ability of ADA-308 to inhibit AR activity in models that have developed resistance to ENZ suggests its potential as an effective agent to follow ARPI resistance. However, while there is potential for ADA-308 in PCa, the commercialization of the program in PCa became challenging for Aranda Pharma Ltd. due to changes in clinical practice (such as the sequential use of second-generation AR inhibitors is not recommended when one fails) and high competition in the market.

Acknowledgements

We thank all the members of the Zoubeidi laboratory (University of British Columbia, Vancouver, Canada) for their valuable input in designing and progressing this research. Specifically, Dr Dwaipayan Ganguli for performing peak calling, quality control, annotation and visualization of the ChIP-seq data and Dr Joshua Scurl for RNA-seq processing and quality control. We also thank the Biomedical Research Centre Sequencing Core (University of British Columbia, Vancouver, Canada) for the RNA-seq processing and the Animal Core Facility (Vancouver Prostate Centre, Vancouver, Canada) for the animal study.

Funding

This research was supported by funding from Aranda Pharma Ltd as well as the Prostate Cancer Foundation Young Investigator Award (to SN).

Availability of data and materials

The RNA-seq data generated in the present study may be found in the GEO database under the accession no. GSE267309 or at the following URL: <https://www.ncbi.nlm.nih.gov/geo/query/acc.cgi?acc=GSE267309>. All other data generated in the present study may be requested from the corresponding author.

Authors' contributions

SN, FJ, SK, OS, NT, MK, AM and AZ confirm the authenticity of all the raw data, conceived this study and took responsibility for the quality of the data. AM and MK contributed to the study design. AM, SN and FJ participated in the analysis and interpretation of data and prepared all figures. FJ and SK

performed all the *in vitro* experiments and acquired data. NT performed the proliferation assay and assisted in the revision of this manuscript. OS performed the *in vivo* experiments. SN wrote the manuscript. AZ, AM and FJ reviewed and edited the manuscript. All authors read and approved the final version of the manuscript.

Ethics approval and consent to participate

All animal experiments were performed in accordance with the procedures and protocols of the Laboratory Animal Center of the University of British Columbia (Vancouver, Canada; approval no. A16-0246; approval date, 12/15/2016).

Patient consent for publication

Not applicable.

Competing interests

Aranda Pharma Ltd. owns the IP of ADA-308. AM and MK are shareholders of Aranda Pharma Ltd. All other authors declare that they have no competing interests.

References

- Bergengren O, Pekala KR, Matsoukas K, Fainberg J, Mungovan SF, Bratt O, Bray F, Brawley O, Luckenbaugh AN, Mucci L, *et al*: 2022 Update on prostate cancer epidemiology and risk factors-a systematic review. *Eur Urol* 84: 191-206, 2023.
- Zhang W, Cao G, Wu F, Wang Y, Liu Z, Hu H and Xu K: Global burden of prostate cancer and association with socioeconomic status, 1990-2019: A systematic analysis from the global burden of disease study. *J Epidemiol Glob Health* 13: 407-421, 2023.
- World Health Organization (WHO): Prostate cancer statistics. WHO, Geneva, 2024.
- Heinlein CA and Chang C: Androgen receptor in prostate cancer. *Endocr Rev* 25: 276-308, 2004.
- Seikkula H, Boström PJ, Seppä K, Pitkaniemi J, Malila N and Kaipia A: Survival and mortality of elderly men with localized prostate cancer managed with primary androgen deprivation therapy or by primary observation. *BMC Urol* 20: 25, 2020.
- Kokorovic A, So AI, Serag H, French C, Hamilton RJ, Izard JP, Nayak JG, Pouliot F, Saad F, Shayegan B, *et al*: Canadian urological association guideline on androgen deprivation therapy: Adverse events and management strategies. *Can Urol Assoc J* 15: E307-E322, 2021.
- Vellky JE and Ricke WA: Development and prevalence of castration-resistant prostate cancer subtypes. *Neoplasia* 22: 566-575, 2020.
- Kirby M, Hirst C and Crawford ED: Characterising the castration-resistant prostate cancer population: A systematic review. *Int J Clin Pract* 65: 1180-1192, 2011.
- Scher HI, Fizazi K, Saad F, Taplin ME, Sternberg CN, Miller K, de Wit R, Mulders P, Chi KN, Shore ND, *et al*: Increased survival with enzalutamide in prostate cancer after chemotherapy. *N Engl J Med* 367: 1187-1197, 2012.
- de Bono JS, Logothetis CJ, Molina A, Fizazi K, North S, Chu L, Chi KN, Jones RJ, Goodman OB Jr, Saad F, *et al*: Abiraterone and increased survival in metastatic prostate cancer. *N Engl J Med* 364: 1995-2005, 2011.
- Nevedomskaya E, Baumgart SJ and Haendler B: Recent advances in prostate cancer treatment and drug discovery. *Int J Mol Sci* 19: 1359, 2018.
- Mateo J, Smith A, Ong M and de Bono JS: Novel drugs targeting the androgen receptor pathway in prostate cancer. *Cancer Metastasis Rev* 33: 567-579, 2014.
- Crona DJ, Milowsky MI and Whang YE: Androgen receptor targeting drugs in castration-resistant prostate cancer and mechanisms of resistance. *Clin Pharmacol Ther* 98: 582-589, 2015.
- Abida W, Cyrta J, Heller G, Prandi D, Armenia J, Coleman I, Cieslik M, Benelli M, Robinson D, Van Allen EM, *et al*: Genomic correlates of clinical outcome in advanced prostate cancer. *Proc Natl Acad Sci USA* 116: 11428-11436, 2019.
- Arora VK, Schenkein E, Murali R, Subudhi SK, Wongvipat J, Balbas MD, Shah N, Cai L, Efsthathiou E, Logothetis C, *et al*: Glucocorticoid receptor confers resistance to antiandrogens by bypassing androgen receptor blockade. *Cell* 155: 1309-1322, 2013.
- Antonarakis ES, Lu C, Wang H, Luber B, Nakazawa M, Roeser JC, Chen Y, Mohammad TA, Chen Y, Fedor HL, *et al*: AR-V7 and resistance to enzalutamide and abiraterone in prostate cancer. *N Engl J Med* 371: 1028-1038, 2014.
- Cato L, de Tribolet-Hardy J, Lee I, Rottenberg JT, Coleman I, Melchers D, Houtman R, Xiao T, Li W, Uo T, *et al*: ARv7 represses tumor-suppressor genes in castration-resistant prostate cancer. *Cancer Cell* 35: 401-413.e6, 2019.
- Joseph JD, Lu N, Qian J, Sensintaffar J, Shao G, Brigham D, Moon M, Maneval EC, Chen I, Darimont B and Hager JH: A clinically relevant androgen receptor mutation confers resistance to second-generation antiandrogens enzalutamide and ARN-509. *Cancer Discov* 3: 1020-1029, 2013.
- Einstein DJ, Arai S and Balk SP: Targeting the androgen receptor and overcoming resistance in prostate cancer. *Curr Opin Oncol* 31: 175-182, 2019.
- Takeda DY, Spisák S, Seo JH, Bell C, O'Connor E, Korthauer K, Ribli D, Csabai I, Solymosi N, Szállási Z, *et al*: A somatically acquired enhancer of the androgen receptor is a noncoding driver in advanced prostate cancer. *Cell* 174: 422-432.e13, 2018.
- Quigley DA, Dang HX, Zhao SG, Lloyd P, Aggarwal R, Alumkal JJ, Foye A, Kothari V, Perry MD, Bailey AM, *et al*: Genomic hallmarks and structural variation in metastatic prostate cancer. *Cell* 175: 889, 2018.
- Viswanathan SR, Ha G, Hoff AM, Wala JA, Carrot-Zhang J, Whelan CW, Haradhvala NJ, Freeman SS, Reed SC, Rhoades J, *et al*: Structural alterations driving castration-resistant prostate cancer revealed by linked-read genome sequencing. *Cell* 174: 433-447.e19, 2018.
- Blum EG, Coleman IM, Lucas JM, Coleman RT, Hernandez-Lopez S, Tharakan R, Bianchi-Frias D, Dumpit RF, Kaipainen A, Corella AN, *et al*: Androgen receptor pathway-independent prostate cancer is sustained through FGF signaling. *Cancer Cell* 32: 474-489.e6, 2017.
- Li Q, Deng Q, Chao HP, Liu X, Lu Y, Lin K, Liu B, Tang GW, Zhang D, Tracz A, *et al*: Linking prostate cancer cell AR heterogeneity to distinct castration and enzalutamide responses. *Nat Commun* 9: 3600, 2018.
- He Y, Wei T, Ye Z, Orme JJ, Lin D, Sheng H, Fazli L, Jeffrey Karnes R, Jimenez R, Wang L, *et al*: A noncanonical AR addiction drives enzalutamide resistance in prostate cancer. *Nat Commun* 12: 1521, 2021.
- Davies A, Nouruzi S, Ganguli D, Namekawa T, Thaper D, Linder S, Karaoglanoglu F, Omur ME, Kim S, Kobelev M, *et al*: An androgen receptor switch underlies lineage infidelity in treatment-resistant prostate cancer. *Nat Cell Biol* 23: 1023-1034, 2021.
- Moilanen AM, Riikonen R, Oksala R, Ravanti L, Aho E, Wohlfahrt G, Nykänen PS, Törmäkangas OP, Palmio JJ and Kallio PJ: Discovery of ODM-201, a new-generation androgen receptor inhibitor targeting resistance mechanisms to androgen signaling-directed prostate cancer therapies. *Sci Rep* 5: 12007, 2015.
- Bishop JL, Thaper D, Vahid S, Davies A, Ketola K, Kuruma H, Jama R, Nip KM, Angeles A, Johnson F, *et al*: The master neural transcription factor BRN2 is an androgen receptor-suppressed driver of neuroendocrine differentiation in prostate cancer. *Cancer Discov* 7: 54-71, 2017.
- Livak KJ and Schmittgen TD: Analysis of relative gene expression data using real-time quantitative PCR and the 2(-Delta Delta C(T)) method. *Methods* 25: 402-408, 2001.
- Yeh S, Kang HY, Miyamoto H, Nishimura K, Chang HC, Ting HJ, Rahman M, Lin HK, Fujimoto N, Hu YC, *et al*: Differential induction of androgen receptor transactivation by different androgen receptor coactivators in human prostate cancer DU145 cells. *Endocrine* 11: 195-202, 1999.
- Dobin A, Davis CA, Schlesinger F, Drenkow J, Zaleski C, Jha S, Batut P, Chaisson M and Gingeras TR: STAR: Ultrafast universal RNA-seq aligner. *Bioinformatics* 29: 15-21, 2013.
- Trapnell C, Roberts A, Goff L, Pertea G, Kim D, Kelley DR, Pimentel H, Salzberg SL, Rinn JL and Pachter L: Differential gene and transcript expression analysis of RNA-seq experiments with TopHat and cufflinks. *Nat Protoc* 7: 562-578, 2012.

33. Love MI, Huber W and Anders S: Moderated estimation of fold change and dispersion for RNA-seq data with DESeq2. *Genome Biol* 15: 550, 2014.
34. Chen Z, Lan X, Thomas-Ahner JM, Wu D, Liu X, Ye Z, Wang L, Sunkel B, Grenade C, Chen J, *et al*: Agonist and antagonist switch DNA motifs recognized by human androgen receptor in prostate cancer. *EMBO J* 34: 502-516, 2015.
35. Bittencourt SA: FastQC: A quality control tool for high throughput sequence data. Babraham Bioinformatics, 2010.
36. Li H and Durbin R: Fast and accurate short read alignment with Burrows-Wheeler transform. *Bioinformatics* 25: 1754-1760, 2009.
37. Li H, Handsaker B, Wysoker A, Fennell T, Ruan J, Homer N, Marth G, Abecasis G and Durbin R; 1000 Genome Project Data Processing Subgroup: The sequence alignment/map format and SAMtools. *Bioinformatics* 25: 2078-2079, 2009.
38. Zhang Y, Liu T, Meyer CA, Eeckhoutte J, Johnson DS, Bernstein BE, Nusbaum C, Myers RM, Brown M, Li W and Liu XS: Model-based analysis of ChIP-Seq (MACS). *Genome Biol* 9: R137, 2008.
39. Ramirez F, Ryan DP, Grüning B, Bhardwaj V, Kilpert F, Richter AS, Heyne S, Dündar F and Manke T: deepTools2: A next generation web server for deep-sequencing data analysis. *Nucleic Acids Res* 44: W160-W165, 2016.
40. Quinlan AR and Hall IM: BEDTools: A flexible suite of utilities for comparing genomic features. *Bioinformatics* 26: 841-842, 2010.
41. Reimand J, Arak T, Adler P, Kolberg L, Reisberg S, Peterson H and Vilo J: g:Profiler-a web server for functional interpretation of gene lists (2016 update). *Nucleic Acids Res* 44: W83-W89, 2016.
42. Subramanian A, Tamayo P, Mootha VK, Mukherjee S, Ebert BL, Gillette MA, Paulovich A, Pomeroy SL, Golub TR, Lander ES and Mesirov JP: Gene set enrichment analysis: A knowledge-based approach for interpreting genome-wide expression profiles. *Proc Natl Acad Sci USA* 102: 15545-15550, 2005.
43. Maffey AH, Ishibashi T, He C, Wang X, White AR, Hendy SC, Nelson CC, Rennie PS and Ausió J: Probasin promoter assemblies into a strongly positioned nucleosome that permits androgen receptor binding. *Mol Cell Endocrinol* 268: 10-19, 2007.
44. Namekawa T, Ikeda K, Horie-Inoue K and Inoue S: Application of prostate cancer models for preclinical study: Advantages and limitations of cell lines, patient-derived xenografts, and three-dimensional culture of patient-derived cells. *Cells* 8: 74, 2019.
45. Borgmann H, Lallous N, Ozistanbullu D, Beraldi E, Paul N, Dalal K, Fazli L, Haferkamp A, Lejeune P, Cherkasov A and Gleave ME: Moving towards precision urologic oncology: Targeting enzalutamide-resistant prostate cancer and mutated forms of the androgen receptor using the novel inhibitor darolutamide (ODM-201). *Eur Urol* 73: 4-8, 2018.
46. Waltering KK, Urbanucci A and Visakorpi T: Androgen receptor (AR) aberrations in castration-resistant prostate cancer. *Mol Cell Endocrinol* 360: 38-43, 2012.
47. Korpala M, Korn JM, Gao X, Rakiec DP, Ruddy DA, Doshi S, Yuan J, Kovats SG, Kim S, Cooke VG, *et al*: An F876L mutation in androgen receptor confers genetic and phenotypic resistance to MDV3100 (enzalutamide). *Cancer Discov* 3: 1030-1043, 2013.
48. Liu H, Wang L, Tian J, Li J and Liu H: Molecular dynamics studies on the enzalutamide resistance mechanisms induced by androgen receptor mutations. *J Cell Biochem* 118: 2792-2801, 2017.
49. Veldscholte J, Ris-Stalpers C, Kuiper GG, Jenster G, Berrevoets C, Claassen E, van Rooij HC, Trapman J, Brinkmann AO and Mulder E: A mutation in the ligand binding domain of the androgen receptor of human LNCaP cells affects steroid binding characteristics and response to anti-androgens. *Biochem Biophys Res Commun* 173: 534-540, 1990.
50. Dai C, Heemers H and Sharifi N: Androgen signaling in prostate cancer. *Cold Spring Harb Perspect Med* 7: a030452, 2017.
51. Eder IE, Culig Z, Putz T, Nessler-Menardi C, Bartsch G and Klocker H: Molecular biology of the androgen receptor: From molecular understanding to the clinic. *Eur Urol* 40: 241-251, 2001.
52. Smith DF and Toft DO: Minireview: The intersection of steroid receptors with molecular chaperones: Observations and questions. *Mol Endocrinol* 22: 2229-2240, 2008.
53. Verrijdt G, Haelens A and Claessens F: Selective DNA recognition by the androgen receptor as a mechanism for hormone-specific regulation of gene expression. *Mol Genet Metab* 78: 175-185, 2003.
54. Zhao J, Zhao Y, Wang L, Zhang J, Karnes RJ, Kohli M, Wang G and Huang H: Alterations of androgen receptor-regulated enhancer RNAs (eRNAs) contribute to enzalutamide resistance in castration-resistant prostate cancer. *Oncotarget* 7: 38551-38565, 2016.
55. Li K, Guo Y, Yang X, Zhang Z, Zhang C and Xu Y: ELF5-mediated AR activation regulates prostate cancer progression. *Sci Rep* 7: 42759, 2017.
56. Rodriguez-Vida A, Galazi M, Rudman S, Chowdhury S and Sternberg CN: Enzalutamide for the treatment of metastatic castration-resistant prostate cancer. *Drug Des Devel Ther* 9: 3325-3339, 2015.
57. Ryan CJ, Smith MR, de Bono JS, Molina A, Logothetis CJ, de Souza P, Fizazi K, Mainwaring P, Piulats JM, Ng S, *et al*: Abiraterone in metastatic prostate cancer without previous chemotherapy. *N Engl J Med* 368: 138-148, 2013.
58. Fizazi K, Scher HI, Molina A, Logothetis CJ, Chi KN, Jones RJ, Staffurth JN, North S, Vogelzang NJ, Saad F, *et al*: Abiraterone acetate for treatment of metastatic castration-resistant prostate cancer: Final overall survival analysis of the COU-AA-301 randomised, double-blind, placebo-controlled phase 3 study. *Lancet Oncol* 13: 983-992, 2012.
59. Mostaghel EA, Marck BT, Plymate SR, Vessella RL, Balk S, Matsumoto AM, Nelson PS and Montgomery RB: Resistance to CYP17A1 inhibition with abiraterone in castration-resistant prostate cancer: Induction of steroidogenesis and androgen receptor splice variants. *Clin Cancer Res* 17: 5913-5925, 2011.
60. Locke JA, Guns ES, Lubik AA, Adomat HH, Hendy SC, Wood CA, Ettinger SL, Gleave ME and Nelson CC: Androgen levels increase by intratumoral de novo steroidogenesis during progression of castration-resistant prostate cancer. *Cancer Res* 68: 6407-6415, 2008.
61. Montgomery RB, Mostaghel EA, Vessella R, Hess DL, Kalhorn TF, Higano CS, True LD and Nelson PS: Maintenance of intratumoral androgens in metastatic prostate cancer: A mechanism for castration-resistant tumor growth. *Cancer Res* 68: 4447-4454, 2008.
62. Lallous N, Dalal K, Cherkasov A and Rennie PS: Targeting alternative sites on the androgen receptor to treat castration-resistant prostate cancer. *Int J Mol Sci* 14: 12496-12519, 2013.
63. Nouruzi S, Ganguli D, Tabrizian N, Kobelev M, Sivak O, Namekawa T, Thaper D, Baca SC, Freedman ML, Aguda A, *et al*: ASCL1 activates neuronal stem cell-like lineage programming through remodeling of the chromatin landscape in prostate cancer. *Nat Commun* 13: 2282, 2022.
64. Tabrizian N, Nouruzi S, Cui CJ, Kobelev M, Namekawa T, Lodhia I, Talal A, Sivak O, Ganguli D and Zoubeidi A: ASCL1 is activated downstream of the ROR2/CREB signaling pathway to support lineage plasticity in prostate cancer. *Cell Rep* 42: 112937, 2023.
65. Beltran H, Hruszkewycz A, Scher HI, Hildesheim J, Isaacs J, Yu EY, Kelly K, Lin D, Dicker A, Arnold J, *et al*: The role of lineage plasticity in prostate cancer therapy resistance. *Clin Cancer Res* 25: 6916-6924, 2019.
66. Beltran H, Prandi D, Mosquera JM, Benelli M, Puca L, Cyrta J, Marotz C, Giannopoulou E, Chakravarthi BV, Varambally S, *et al*: Divergent clonal evolution of castration-resistant neuroendocrine prostate cancer. *Nat Med* 22: 298-305, 2016.
67. Aggarwal R, Huang J, Alumkal JJ, Zhang L, Feng FY, Thomas GV, Weinstein AS, Friedl V, Zhang C, Witte ON, *et al*: Clinical and genomic characterization of treatment-emergent small-cell neuroendocrine prostate cancer: A multi-institutional prospective study. *J Clin Oncol* 36: 2492-2503, 2018.
68. Linder S, Hoogstraat M, Stelloo S, Eickhoff N, Schuurman K, de Barros H, Alkemade M, Bekers EM, Severson TM, Sanders J, *et al*: Drug-induced epigenomic plasticity reprograms circadian rhythm regulation to drive prostate cancer toward androgen independence. *Cancer Discov* 12: 2074-2097, 2022.

